

LNF-11/04 (P)
April 7, 2011

ANALYSIS OF RELATIVISTIC PROTON DEFLECTION BY BENT CRYSTALS

A. Babaev, and S.B. Dabagov
Laboratori Nazionali di Frascati, Italy

Abstract

The peculiarities of the motion of charged particles through the bent crystals open wide possibilities to manipulate charge particle beams. Namely, bent crystal techniques allow deflecting and separating the particles on dependence of their energies. In this manuscript simulations for the deflection of relativistic proton beam by bent crystallographic planes are presented; our simulations are based on the numerical solution of the equation for radial proton motion.

PACS.: 61.85.+p – bent crystal, volume reflection

Presented at 4th International Conference on Charged & Neutral Particles Channeling
Phenomena - Channeling 2010 (October 3-8, 2010, Ferrara)

*Published by
Servizio Informazione e Documentazione Scientifica dei LNF
Ufficio Biblioteca e Pubblicazioni*

1. INTRODUCTION

The use of bent crystals to manipulate a charge particle beam was first suggested by Tsyganov in 1976 [1]. At present bent crystal technique is of great interest as one of the accelerator techniques ([2-4] and references therein). Simultaneously with the technique application, the theoretical background for the beam propagation in bent crystallographic channels has been developed [2,5-9]. In this work we follow mainly the earlier model [5,6], but with some essential distinctions. In particular, our approximation does not need to integrate the proton motion equations.

Our main goal was to develop a new computer code to simulate main features of relativistic protons/ions scattering in the field of crystallographic potentials of bent crystals. We tested this code to describe the experimental results [10], in which the motion of 400 GeV proton beam through Si (220) bent crystal has been investigated. In this manuscript we present the deflection of such protons by both a single bent planar channel and a set of bent planes, as well as by real bent crystal. Finally, the angular distributions of protons in the outgoing beam are obtained. The angular divergence of initial proton beam is taken into account also.

2. PLANAR POTENTIAL OF A BENT CRYSTAL AND PROTON MOTION EQUATION

Let the crystal be bent with the radius R . In this case the continuous planar potential of crystallographic planes under consideration is axial. The motion of the proton, which penetrates into the bent crystal under small angle to the crystallographic planes, is managed by the averaged planar potential and the proton trajectory has in general complicated form. In dependence on the initial point of the trajectory, the proton can be captured in the planar channeling regime and it either follows the bent planes (proper channeling), or undergoes the quasi-channeling mode in transverse plane. In this case proton is not constrained with one planar channel. In both cases a simple geometrical consideration can be applied to define the angle of deflection from the initial direction (fig. 1).

Azimuthal velocity $v_\varphi = v_0 \cos \theta_0$ of the proton in this field is constant. On the contrary, the evolution of proton radial velocity v_r is defined by the motion equation [5,6]:

$$\gamma m \frac{dv_r}{dt} = -\frac{dU_{cr}}{dr} + F_C, \quad (1)$$

where γ is the relativistic factor, and m is the rest mass of the proton; U_{cr} is the crystal planar potential (simulations were done within Molier approximation for the potential of interaction); F_C is the centrifugal force determined by the expression:

$$F_C = \frac{E_{kin} + mc^2}{R} \frac{v_0^2}{c^2}, \quad (2)$$

where E_{kin} is the kinetic proton energy, c is the speed of light.

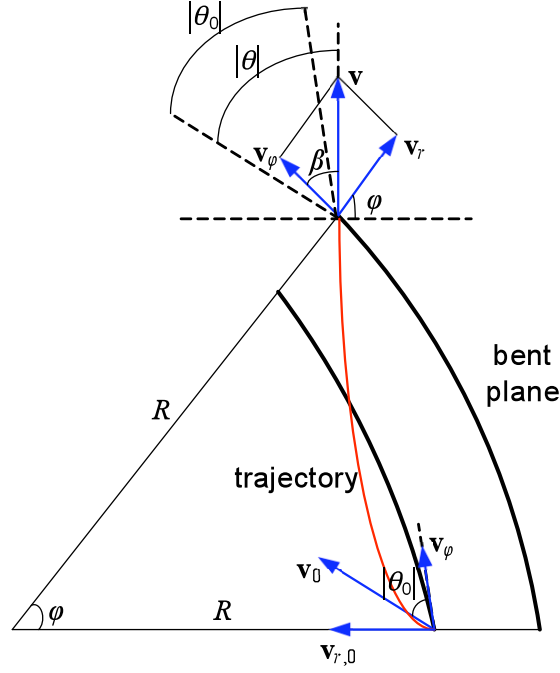


Figure 1. Scheme of the proton motion in a bent crystal.

As the radial coordinate r is counted from the center of curvature, we have $v_r < 0$ when proton moves to the center of curvature, and $v_r > 0$ in opposite case. Hence, it is convenient to establish $\theta_0 < 0$ if the proton moves to the center of curvature and $\theta_0 > 0$ in opposite case, and this choice is in agreement with the sign of β - angle between the proton velocity \mathbf{v} and its azimuthal velocity \mathbf{v}_{φ} in the arbitrary point of trajectory (fig. 1):

$$\operatorname{tg} \beta = \frac{v_r}{v_{\varphi}}. \quad (3)$$

Finally, if the proton angular path is φ , the deflection angle θ from the initial motion direction can be obtained from the formula

$$\theta = \beta - \varphi - \theta_0, \quad (4)$$

where the β angle (3) is evaluated for the final point of trajectory and the radial velocity v_r is defined numerically from the differential equation (1). The suggested method for the deflection angle calculation does not involve the integration of the motion equation and this fact, perhaps, may be attractive for the code applications. Obviously, the fact, that $\theta < 0$, means that proton is deflected to the center of curvature, and from the center in the case $\theta > 0$.

Actually, one can see from Eq.(1) that the radial motion of the proton can be presented as a motion in the effective potential (fig. 2) [5,6]

$$U_{\text{eff}}(r) = U_{\text{cr}}(r) - F_C r + \text{const}. \quad (5)$$

The effective radial potential is characterized by the fact that left and right barriers (see, in fig. 2) of the channel have different heights. This feature explains the motion of the proton in the bent crystal. The character of the proton motion is defined by its radial energy at the initial point of the trajectory

$$E_{r,0} = U_0 + E_{\text{kin},r,0}, \quad (5)$$

U_0 is the potential energy at the initial point of the trajectory concerning the minimum of the potential in the corresponding channel, $E_{\text{kin},r,0}$ is the initial radial kinetic energy

$$E_{\text{kin},r,0} = \frac{1}{2} (E_{\text{kin}} + mc^2) \frac{v_0^2}{c^2} \sin^2 \theta_0. \quad (6)$$

Obviously, the initial radial energy depends on the point of its penetration into the channel. If the proton has the initial radial energy $E_{r,0} < U_{\text{right}}$ (smaller barrier limiting the channel, fig. 2), the proton is captured in the channeling regime. If the proton has the initial radial energy $E_{r,0} > U_{\text{right}}$,

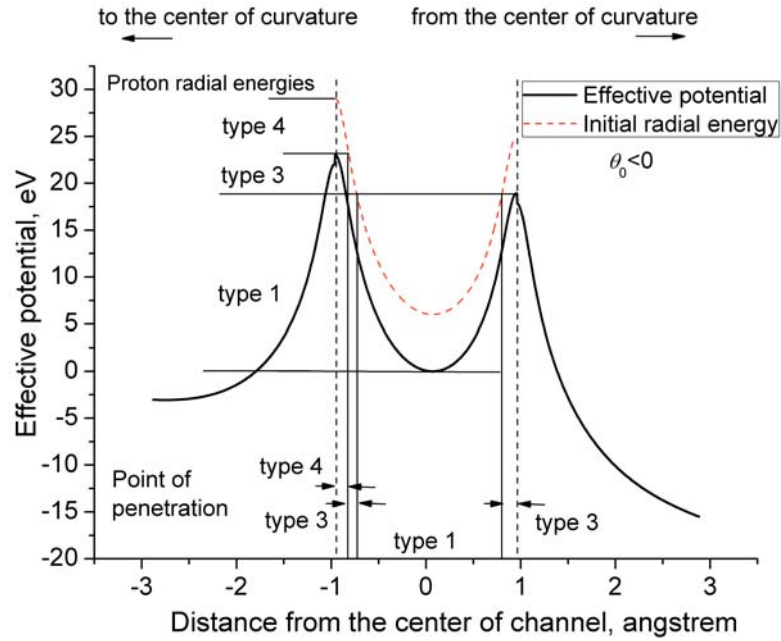


Figure 3. The effective potential of a single planar channel; 400 GeV protons, (220) Si bent channel with radius $R=1852$ cm. Regions corresponding to possible types of trajectories are shown at $\theta_0 < 0$: type 1 corresponds to channeled protons, type 3 – reflected protons, type 4 – protons, which leave the channel above the higher barrier.

In fig. 4 the results of deflection angle simulations are presented at the different angles θ_0 . Here one can see all types of the trajectories pointed out above. The channeled fraction is presented for all situations in fig. 4. These protons are deflected at angles $\theta \approx -\alpha$. In fig. 4a protons penetrating into the channel near the barriers move to the right barrier (see in fig. 3) and leave the channel (type 2); the deflection angle θ for these protons is not big and $\theta > 0$. In fig. 4b the protons initially move parallel to the planes and its initial radial energy is equal to zero, protons penetrating near the left barrier are deflected from the center of curvature at small angle. Reflected protons appear (type 3) as shown in fig. 4c. Also fig. 4c presents protons penetrating near the left barrier having high initial radial energy and leaving the channel above the left barrier (type 4). In fig. 4d, since the initial radial energy (6) increases in comparison to the case of fig. 4c, protons of the type 4 with high initial radial energy exist near both barriers. The reflected protons for all situations are deflected at enough large angles $\theta \geq 10$ μrad and the deflection angle increases when the angle θ_0 grows by its absolute value.

Finally, it should be mentioned that the protons of type 4 in figs. 4c,d are deflected at the negative angles $\theta < 0$ (to the center of curvature) due to influence of electric field from the left of a channel (see in fig. 3). Similar effects may open new possibilities to manage the particle beam. Nevertheless, in the real crystal with the large number of planes, all protons of type 4 should be reflected by other barriers.

4. PASSAGE OF QUASI-CHANNELED PROTONS THROUGH A SET OF BENT PLANES

Let consider a set of $2N$ bent planes. Deflection angles of channeled protons are the same in all channels. The main interest is to investigate the angular distributions of quasi-channeled protons, i.e. protons of types 2, 3, 4 (see above) in dependence on the initial point of the trajectory. Obviously, the deflection angle must be correlated with the number of planes, that quasi-channeled proton crosses. The inter-planar potential is the same as in figs. 2, and 3. Also, from both right and left of a set the electric field is spread at the distance a , as in fig. 3 outside the channel. As above mentioned, the motion of 400 GeV protons through the set (220) Si bent planes has been simulated ($R=1852$ cm).

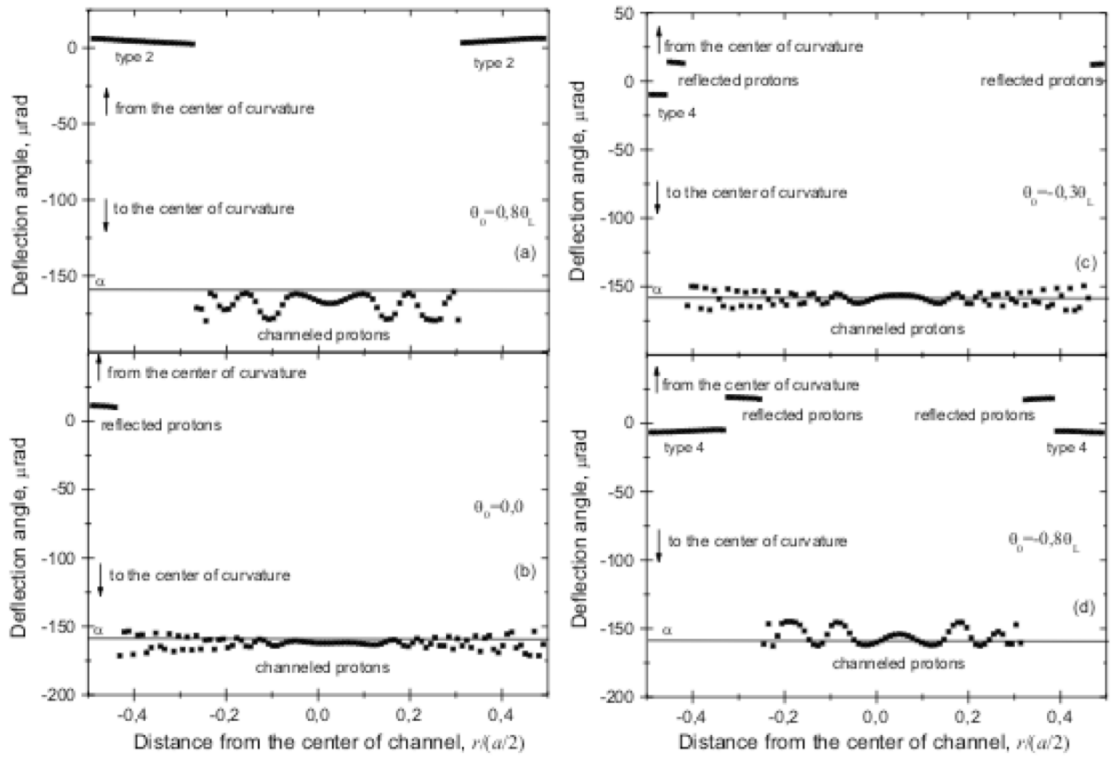


Figure 4. Deflection angles of 400 GeV protons in the single bent (220) Si planar channel at the different angles θ_0 as the function of the point of the penetration into the channel; the radius $R=1852$ cm, crystal bend angle $\alpha=162$ μrad ; a – is the inter-planar distance; the critical channeling angle $\theta_L=10.2$ μrad .

In fig. 5 the deflection angles of quasi-channeled protons are shown at different number of planes $2N$ and different incident angles θ_0 . Since the angles $\theta_0 < 0$ (protons move to the center of curvature initially), here only the trajectories of types 3 (reflected protons) and 4 (non-reflected protons) exist. When protons penetrate parallel to the planes (figs. 5a,c) all protons are deflected at the angles $\theta > 0$, the width of the angular distribution is about 2-3 μrad . In the situation $\theta_0 = -0.8\theta_L$ (figs. 5b,d) protons penetrating into the channels near the inner border of the set (near to the center of curvature) has the large initial radial energy and leave the electric field without reflection, whereas other protons are reflected. Non-reflected protons are deflected at negative angles $\theta \approx -5$ μrad . Reflected protons are deflected at angles $\theta \approx 15$ μrad and this value is about the doubled value at the deflection angle for the protons penetrating at the angle $\theta_0 = 0$ (see the similar conclusion in [5,6]).

Points lying on the smooth growing curve correspond to the same points in the neighboring channels. Following this curve one can watch the evolution of the deflection angle in dependence on the trace of proton (on the number of crossed planes) for given initial point in the channel. Points lying on the almost vertical space correspond to the points in the one channel. The length of the space characterizes the width of the angular distribution of these protons. Protons penetrating to the channels near the outer border of the set (distant from the center of curvature) are reflected at the larger angles than ones penetrating near the inner border. Also the width of the angular distribution for protons penetrating into the one channel near the inner border is larger than the width for protons penetrating into the one channel near the outer border. The rate of the deflection angle increasing at the given point in the channel is slowed down with the growth of the distance from the outer border. These features are shown in all situations in fig. 5. It should be mentioned, that reflected protons penetrating near the inner border pass the larger way (and cross the larger number of planes) through the crystal than ones penetrating near the outer border, and

namely the first protons are deflected at the fewer angles. Moreover, the change of deflection angles stops when the number of planes increases.

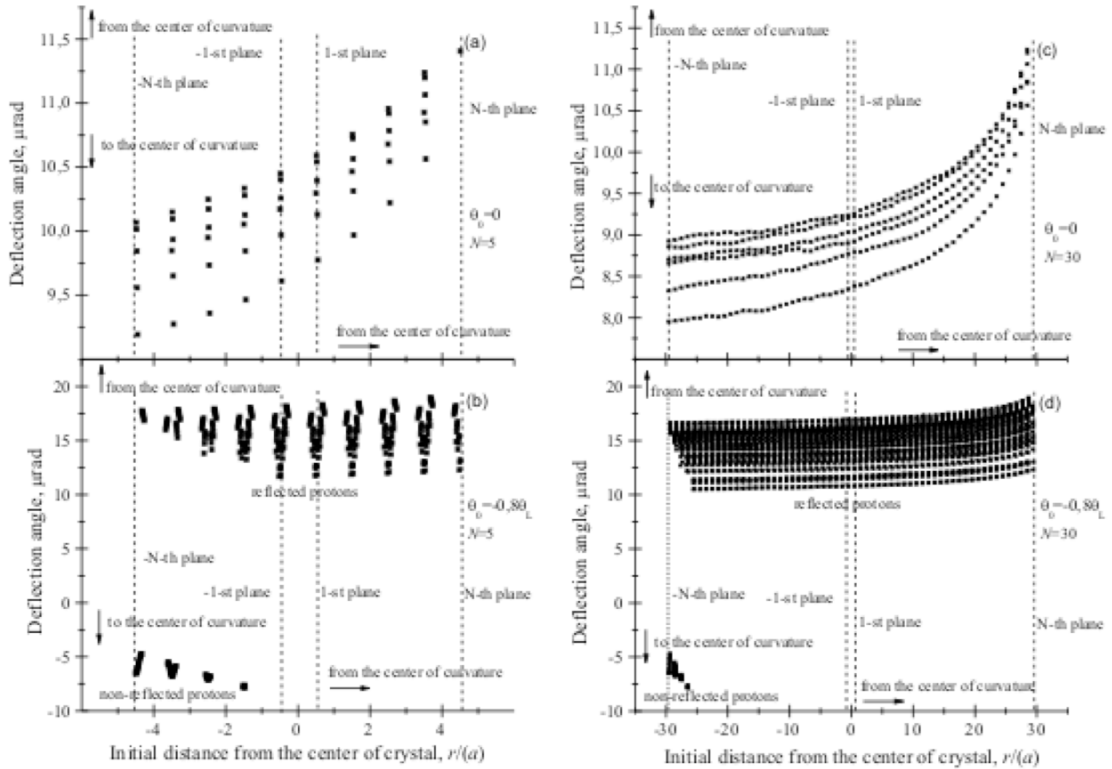


Figure 5. Deflection angles of quasi-channeled 400 GeV protons in the set of $2N$ bent (220) Si planes at different angles θ_0 as a function of the initial distance from the center of a set; the radius of curvature is $R=1852$ cm; a is the inter-planar distance; the critical channeling angle $\theta_L=10.2$ μrad .

Finally, the effect of saturation of the deflection angle when the number of planes is increasing, gives the possibility to take into account for real crystals only small number of planes. Indeed, the real crystal has the width about 1 mm and contains the huge number of the planes – about 10^7 . But the deflection angle value is not change practically, when proton pass about 100 planes (see in figs. 5b,d). Hence, to calculate the deflection angle of quasi-channeled protons it is enough to take into account all planes before the point of reflection and the first 100-200 planes after this point (see the similar conclusion in [5,6]). Also, in the case of the real crystal the contribution in the angular distribution of the non-reflected quasi-channeled protons penetrating into the crystal near its borders will be negligible in comparison to the contribution of reflected protons.

5. PASSAGE OF RELATIVISTIC PROTONS THROUGH A REAL BENT CRYSTAL

A real bent crystal is characterized by huge number of bent planes. Hence, one can neglect protons penetrating into the crystal near the crystal borders, and one can suggest that all protons pass the angular way α (bend angle of a crystal).

In fig. 6 the simulation of deflection angles for 400 GeV protons passing through the (220) Si bent crystal ($R=1852$ cm, $\alpha=162$ μrad) are presented. The effective planar potential of bent crystal is presented in fig. 1. As shown in fig. 6a,b,c at the angles $|\theta_0| \leq \theta_L$ the channeled protons fraction exists ($E_{r,0} < U_{\text{right}}$ in fig. 1), these protons are deflected at angles $\theta \sim -\alpha$. In fig. 6a $\theta_0 > 0$ and in the outgoing proton beam the quasi-channeled non-reflected fraction exists ($E_{r,0} > U_{\text{right}}$ in fig. 1), because protons move from the center of curvature initially, as protons of the type 2 in the situa-

tion of the single planar channel (section 3). These protons are deflected slightly at angles $\theta > 0$. In fig. 6b,c at the angles $-\theta_L \leq \theta_0 \leq 0$ the reflected fraction ($E_{r,0} > U_{\text{right}}$ in fig. 1) appears together with the channeled protons. In fig. 6d at the angle $|\theta_0| > \theta_L$ the initial radial energy for all protons is so great, that channeled fraction is absent and all protons are reflected.

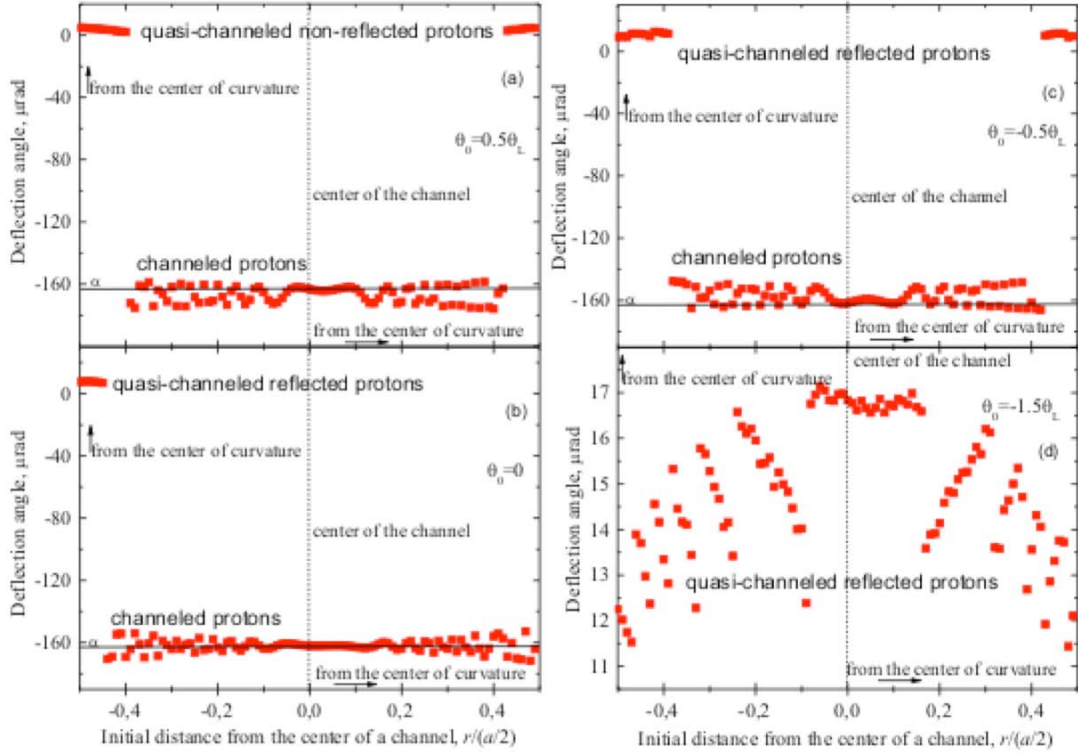


Figure 6. Deflection angles for 400 GeV protons in bent Si (220) crystal at various angles θ_0 as a function of the point of penetration in a channel; the radius of curvature $R=1852$ cm, crystal bend angle $\alpha=162$ μrad ; a is the inter-planar distance; the critical channeling angle $\theta_L=10.2$ μrad .

It should be mentioned (see fig. 6d) that protons having the close initial radial coordinates (and, therefore, close initial radial energies) form groups (inclined spaces at the right and at the left, the horizontal space at the center of the channel) which reflected by one bent plane in the infinity periodical structure.

Let consider 1000 trajectories with uniformly distributed initial points along the channel. The space of deflection angle is divided onto sections at 0.1 μrad width. For each section the number of trajectories is defined, for that the deflection angle θ hits this section. This number of trajectories is pointed out along Y axis, whereas corresponding sections are pointed out along X axis. Hence, obtained histogram presents the angular distributions of protons at given angle θ_0 .

In fig. 7 angular distributions for angles $-\theta_L \leq \theta_0 \leq 0$ are presented. The distribution is divided onto two parts: the channeled and the reflected protons. The channeled protons are deflected along channels at angles $\theta \sim -\alpha$. When the absolute value of angle θ_0 increases (from fig. 7a to fig. 7b), the number of the reflected protons increases due to the increase of the initial radial energy, the distribution of the reflected protons shifts to large angles θ , the width of the reflected protons distribution increases.

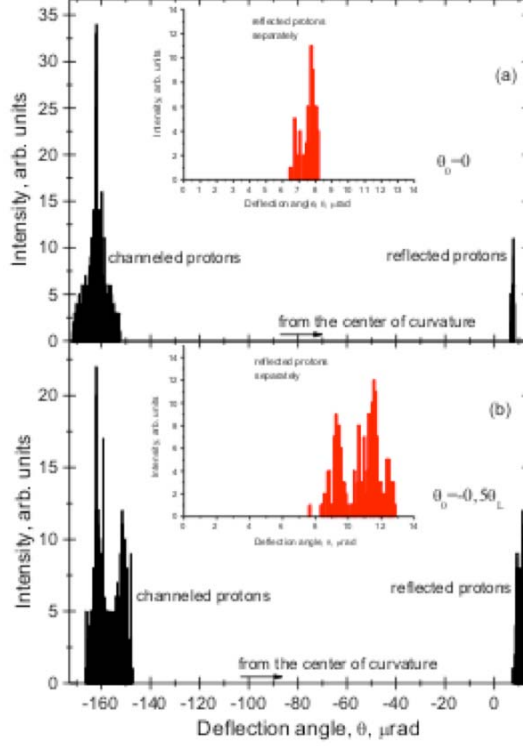


Figure 7. Angular distributions for 400 GeV protons passing through the bent Si (220) crystal at angles $-\theta_L \leq \theta_0 \leq 0$; the curvature radius $R=1852$ cm, crystal bend angle $\alpha=162$ μrad ; the critical channeling angle $\theta_L=10.2$ μrad .

In fig. 8 angular distributions for angles $\theta_0 \leq -\theta_L$ are presented. For these angles only reflected protons exist. When the absolute value of angle θ_0 increases (from fig. 8a to fig. 8d) the angular distributions are narrowed slightly, whereas the edge of distributions at large deflection angles becomes sharper. The common shape of distributions is: the proton intensity increases smoothly from the edge at small deflection angles to the distribution center, where the distribution has the local maximum, after that the distribution has the deep, and finally at large deflection angle the distribution has the pronounced maximum with the distinct edge. This shape is in the agreement with [5,6].

Finally, it should be mentioned that, from the data in fig. 8, the averaged deflection angle at $\theta_0 \leq -\theta_L$, is approximately doubled in comparison with the deflection angle at $\theta_0=0$ (see fig. 7a) in agreement with conclusion of the paper [10].

To correct compare the results of both simulation and experimental data [10], one needs to take into account the initial angular divergence of the proton beam, which equals $\Delta\theta=8\mu\text{rad}$. One can suggest, the initial beam is characterized by the position of the center of beam θ_C and incident angles θ_0 of the protons are distributed uniformly in the interval $(\theta_C - \Delta\theta/2; \theta_C + \Delta\theta/2)$. To take into account the angular divergence the algorithm described above for the single incident angle was repeated for angles in this interval with the step 0.5 μrad . For each incident angle 300 uniformly distributed trajectories were simulated. The space of deflection angles is divided onto sections at 0.1 μrad width. For each section the number of trajectories is defined, for that the deflection angle θ hits this section. This number of trajectories is pointed out along Y axis, whereas corresponding sections are pointed out along X axis. Hence, obtained histogram presents the angular distributions of the protons at given center proton beam angle θ_C .

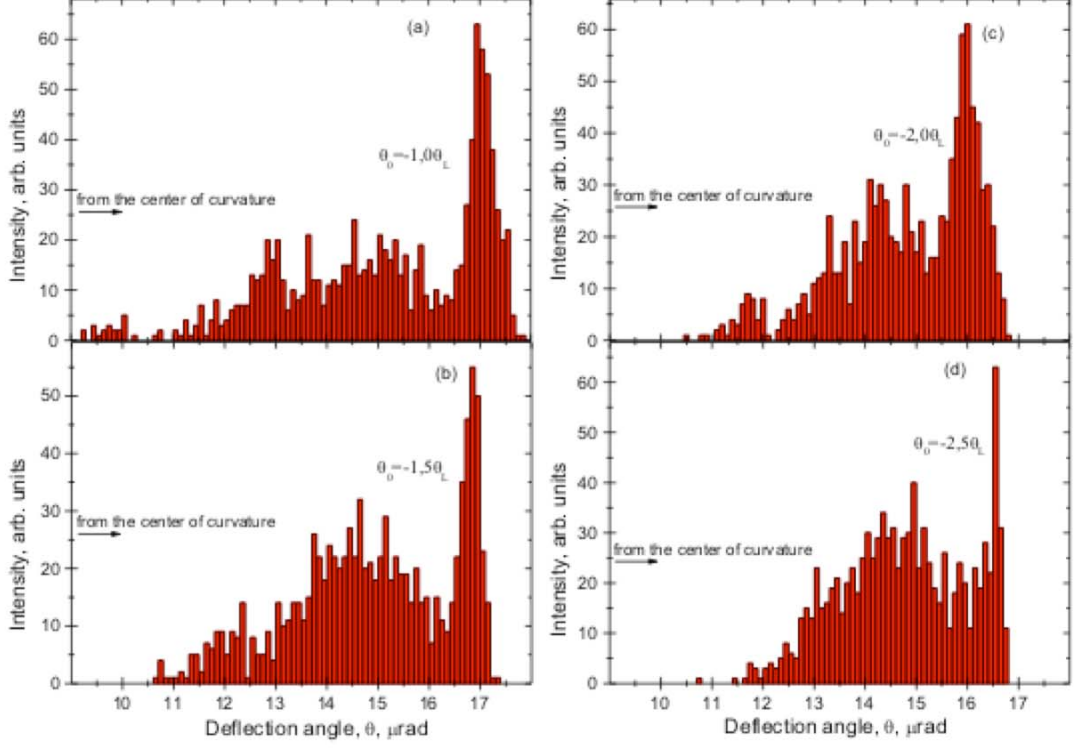


Figure 8. Angular distributions of 400 GeV protons passing through the bent Si (220) crystal at angles $\theta_0 \leq -\theta_L$; the curvature radius $R=1852$ cm, crystal bend angle $\alpha=162$ μrad ; the critical channeling angle $\theta_L=10.2$ μrad .

In fig. 9 the angular distributions for the different angles $\theta_c \leq 0$ are presented. The angle θ_c increases from fig. 9a to fig. 9f. In fig. 9a-c both channeled and reflected fraction exist, even in fig. 9c for $\theta_c = -\theta_L$ whereas in fig. 8a ($\theta_0 = -\theta_L$) the channeled fraction is absent. This fact is due to angular divergence when some protons has the incident angles $|\theta_0| < \theta_L$ and hence these protons are captured in the channeled regime. In general, the channeled fraction is decreased from fig. 9a to fig. 9c whereas the quasi-channeled fraction increases. It should be underlined that in fig. 9a ($\theta_c = 0$) this fraction includes not only reflected protons but also the quasi-channeled non-reflected protons having the incident angles $\theta_0 > 0$ (see in fig. 6a) due to the initial angular divergence. The angular divergence is responsible for the much more width of the angular distributions at $\theta_c = 0$ in comparison with one in fig. 7a ($\theta_0 = 0$). The comparison of angular distributions width in figs. 9b-f with ones in figs. 7,8 at corresponding angles θ_0 shows, that the initial angular divergence does not influence distribution width significantly. In fig. 9d-f only reflected proton fraction exists. It should be mentioned, that edge of the distribution at large deflection angles is spread, becomes less distinct due to the angular divergence in comparison with the corresponding angles θ_0 in fig. 8. Also, the taking into account the angular divergence is the cause that the shape of the distribution changes: the peak near the edge at the large deflection angles decreases and the deep tends to vanish (see in fig. 8), therefore the central local maximum becomes almost equal to the peak at the large deflection angle.

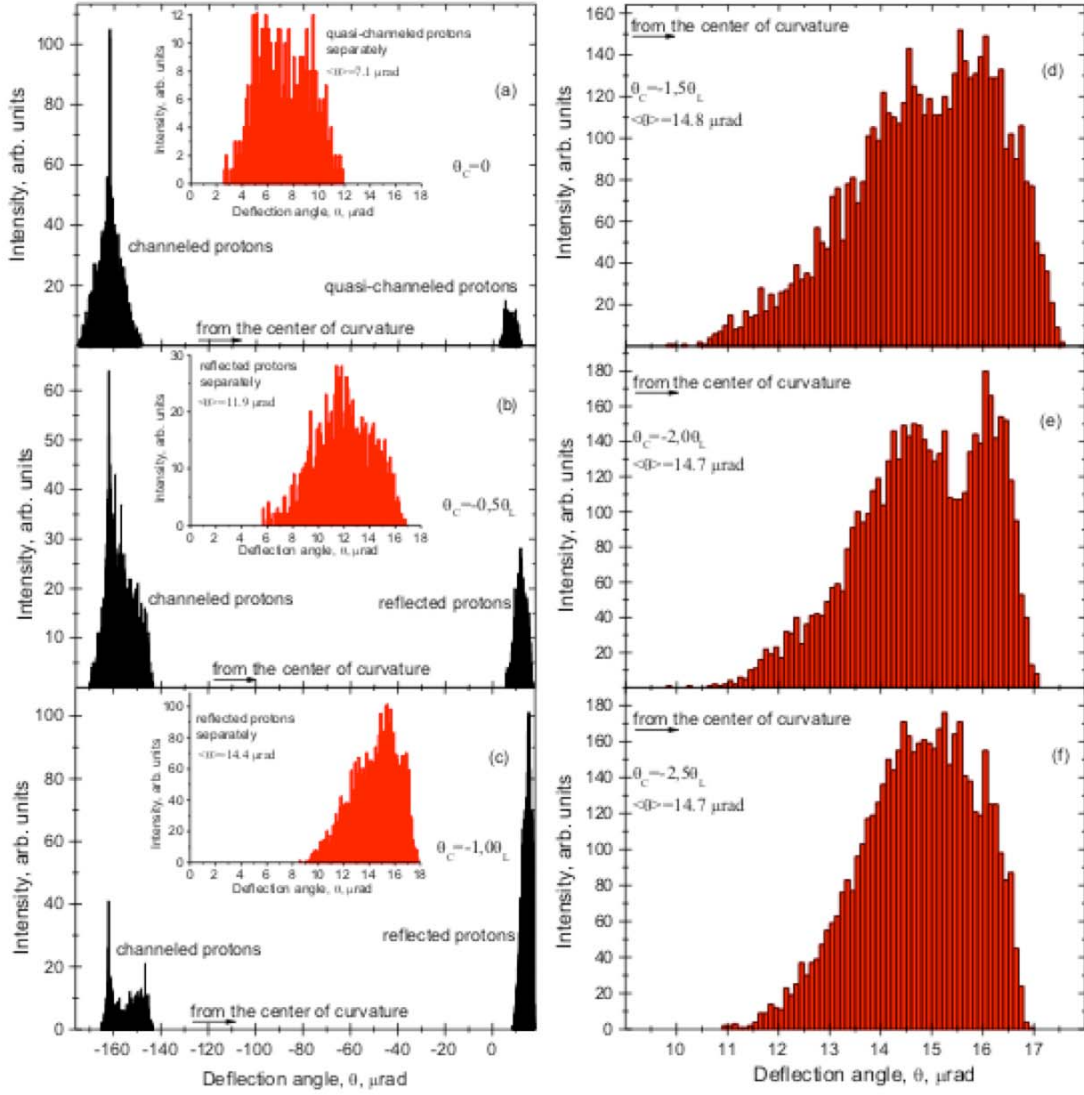


Figure 9. Angular distributions in dependence on angles θ of 400 GeV protons passing through the bent Si (220) crystal at different angles θ_C ; the radius $R=1852$ cm, crystal bend angle $\alpha=162$ μrad ; the critical channeling angle $\theta_L=10.2$ μrad ; the initial angular divergence $\Delta\theta=8\mu\text{rad}$.

It should be underlined that the averaged deflection angle $\langle\theta\rangle$ increases from the $\theta_C=0$ to $\theta_C=-\theta_L$ (from fig. 9a to fig. 9d) and becomes stable for $|\theta_C|\geq\theta_L$. Moreover, the averaged deflection angle is about $\langle\theta\rangle=14.7$ μrad at $\theta_C<-\theta_L$ and this value near to the doubled value of $\langle\theta\rangle$ at $\theta_C=0$ (7.1 μrad).

Nevertheless, the deflection angle θ is not a correct angle for comparison with the experimental data. Indeed, the angle θ is counted from the incident proton direction, but the number of the incident directions exist, when the beam has the initial angular divergence, whereas in the experiment can be measured the angle between the proton motion direction in the outgoing beam and one fixed direction. Hence, let define the angle $\delta=\theta+\theta_0-\theta_C$ for the each trajectory, i. e. the angle δ is the angle between the proton motion direction in the outgoing beam and the direction corresponding to the center of the incident beam. Angular distributions of the protons in dependence on angles δ are shown in fig. 10. All conditions are the same as above, in fig. 9.

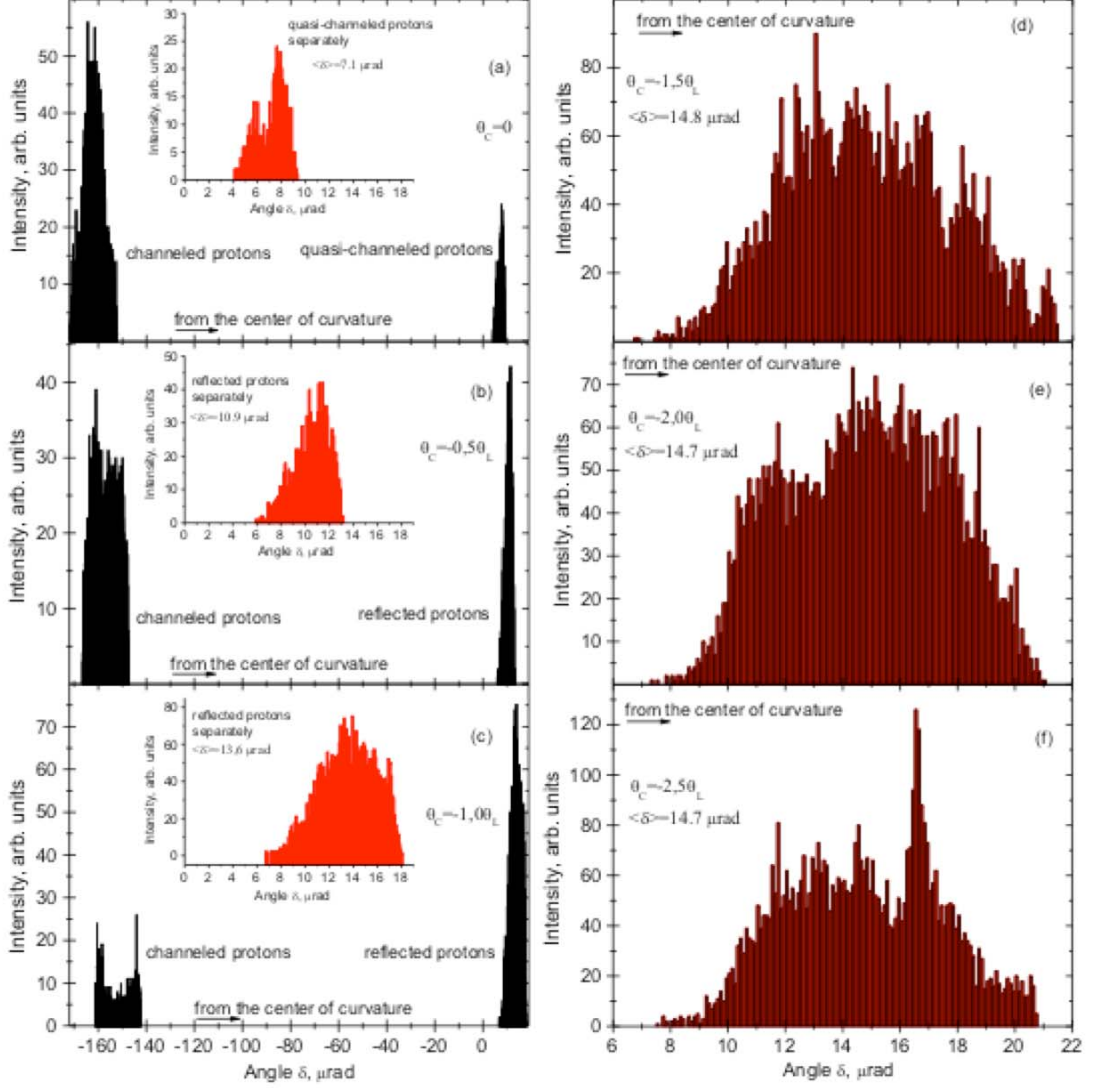


Figure 10. Angular distributions in dependence on angles δ of 400 GeV protons passing through the bent Si (220) crystal at different angles θ_C ; the radius $R=1852$ cm, crystal bend angle $\alpha=162$ μrad ; the critical channeling angle $\theta_L=10.2$ μrad ; the initial angular divergence $\Delta\theta=8$ μrad .

The comparison of figs. 10 and 9 shows that:

1. Angular distributions of channeled protons become broader and magnitudes of the intensity decrease (figs. 9, 10 a-c).
2. Angular distributions of quasi-channeled protons at $\theta_C \leq -0.5\theta_L$ become narrower and magnitudes of the intensity increase (figs. 9, 10 a,b).
3. Angular distributions of quasi-channeled protons at $\theta_C = -\theta_L$ are almost unchanged, only the slight broadening and the small decreasing of magnitudes are found (figs. 9, 10 c).
4. Angular distributions of quasi-channeled protons in figs. 10 a-c have the more distinct edge at the large angles than ones in corresponding fragments in fig. 9.
5. Angular distributions at angles $|\theta_C| \geq \theta_L$ become significantly broader and corresponding magnitudes decrease (figs. 9-10 d-f). In particular, the distinct edge at the large angles δ is fully eliminated.
6. The averaged angles $\langle\theta\rangle$ are the same as corresponding angles $\langle\delta\rangle$ at $|\theta_C| \geq \theta_L$ (figs. 9-10 d-f).

5. CONCLUSION

The simulations presented above were carried out in conditions of previous experiments [10]. The comparison of our calculation results (presented in fig. 10) and this experimental data shows rather good agreement. In particular, the averaged deflection angle of reflected protons at angles $\theta_C < -\theta_L$ is 14.7 μrad , whereas in [10] for this angle the value 13.9 \pm 1.7 μrad is obtained. Width of the distributions of the reflected protons at $\theta_C < -\theta_L$ are in the good agreement with the experimental data also.

The important processes, which are not considered in this manuscript, are due to multiply scattering of projectiles on crystal electrons and nuclei. In the non-oriented case multiply scattering leads to the broadening of the projectile beam. In the condition of this work the multiply scattering not only influence on the width of angular distributions of the outgoing beam protons but it also might cause the new features to be revealed. Namely, these effects are the dechanneling and the volume capture observed in experiments [10].

In future to obtain more realistic picture of the process of proton-bent crystal interaction we will take into account the volume capture and dechanneling effects, which in fact arise due to the change of proton radial energy (this change is connected to the multiply scattering) while it moves in a crystal.

REFERENCES

- [1] E.N. Tsyganov, Fermilab TM-682, TM-684 (1976).
- [2] A.M. Taratin, Physics of Elementary Particles and Atomic Nuclei, **29**, 5 (1998).
- [3] Yu.M. Ivanov, A. A. Petrunin et. al, Phys. Rev. Lett, **97**, 144801 (2006).
- [4] W. Scandale et al., Phys. Rev. Lett, **101**, 234801 (2008).
- [5] A.M. Taratin, and S.A. Vorobiev, Nucl. Instr. Meth. B, **26**, 512 (1987).
- [6] A.M. Taratin, and S.A. Vorobiev, Phys. Lett. A, **119**, 8, 425, (1987).
- [7] V. Biryukov, Phys. Rev. E, **51**, 4, 3522 (1995).
- [8] V.A. Maisheev, Phys. Rev. Special Topics – Accelerators and Beams, **10**, 084701, (2007).
- [9] E. Bagli, V. Guidi, and V.A. Maisheev, Phys. Rev. E, **81**, 026708, (2010).
- [10] W. Scandale et al., Phys. Rev. Lett, **98**, 154801 (2007).